Published in final edited form as:
Eur J Neurosci. 2003 December ; 18(11): 3134–3144.

Structural and Functional Dichotomy of Human Midcingulate Cortex

Brent A. Vogt[1], **Gail R. Berger**[1], and **Stuart W.G. Derbyshire**[2]

1*Cingulum NeuroSciences Institute and Cingulate NeuroTherapeutics, 4435 Stephanie Drive, Manlius, NY 13104*

2*Departments of Anesthesiology and Radiology, University of Pittsburgh Medical Center, Pittsburgh, PA 15213*

Department of Neuroscience and Physiology, SUNY Upstate Medical University, 750 E. Adams Street, Syracuse, NY 13210

Abstract

Anterior cingulate cortex is comprised of perigenual and midcingulate regions based on cytology, imaging, and connections. Its anterior (aMCC) and posterior (pMCC) parts and transition to posterior area 23 were evaluated in 6 human cingulate gyri with Nissl-staining and immunoreactions for neuron-specific nuclear binding protein and intermediate neurofilament proteins (NFP) and their pain and emotion functions evaluated in standard coordinates. Morphological differences included a poorly differentiated layer III with few NFP-expressing neurons in aMCC and a very dense layer Va with small and large pyramids intermingled in pMCC. The density of NFP-positive, layer Vb neurons was higher in pMCC than in aMCC. The junction of pMCC with area 23 had a dysgranular area 23d with clumps of layer IV neurons and a very dense layer Va. Each case was co-registered to standard coordinates and the regional borders identified and measured. Although both regions had overall equivalent activations during noxious cutaneous thermal stimulation, the posterior ⅔ of pMCC was relatively inactive. About 60% of fear-induced activity was in aMCC, sadness and happiness activated perigenual cortex, and neither were activated with non-emotion tasks. Thus, pain activity is coupled to fear in aMCC, while other MCC processing is not related to affect. Beyond midcingulate duality, this is the first report of a very dense layer Va for areas p24' and 23 and the features of transitional area 23d. The MCC dichotomy suggests that two circuits differentially regulate the two cingulate motor areas and involvement of aMCC in pain and fear make it selectively vulnerable to chronic pain and stress syndromes.

Keywords

cytology; cortical lamination; neurofilament proteins; pain; emotion

Use of Brodmann's map in a standardized human brain (Talairach and Tournoux, 1988) led to wide acceptance of this view of cortical organization. The nomenclature, however, was not based on the histology of the atlas case, the original map poorly represented sulcal areas on

Correspondence to Brent A. Vogt, Ph.D., *Cingulum NeuroSciences Institute*, 4435 Stephanie Drive, Manlius, NY 13104, 315-682-0707 bvogt@twcny.rr.com.

Note on terminology: The designations aMCC and pMCC provide a regional terminology for ease of general discussion; however, a unique identifier is needed for each cytological area. Since "'" identifies any area in MCC like area 24b', a means of identifying each area in both parts of MCC is required and an "a" or "p" antecedent is provided. For example, area a24b' refers to the anterior division of area 24b' in MCC and p24b' refers to its posterior part, while area 24b is a division of pACC.

the convoluted surface and many areas were not cytologically uniform. A histological study of area 2 recently assessed postmortem brains with magnetic resonance imaging (Grefkes et al., 2002) and emphasizes an important direction for standardizing regions of interest based on their cytology. In addition, many cytological studies show heterogeneity of Brodmann areas (1909). Midcingulate cortex (MCC), for example, is the posterior part of areas 24 and 32 and areas 24 and 23 have dorsoventral subdivisions (Vogt, 1993; Vogt et al., 1995, 2003). In terms of connections, MCC receives more inferior parietal and less amygdala input than does the perigenual cortex (Vogt and Pandya, 1987) and MCC contains the cingulate motor areas (CMAs), including the primitive gigantopyramidal field of Braak (1976; Matelli et al., 1991; Zilles et al., 1995; Vogt et al., 1995). The CMAs have high densities of glutamate, muscarinic M1, serotonin 1, and α-adrenoceptors compared to the supplementary motor areas (Zilles et al., 1995; Roland and Zilles, 1996). In addition, the CMAs project directly to the spinal cord (Dum and Strick, 1993) and motor cortices (Morecraft and Van Hoesen, 1998; Van Hoesen et al., 1993) and they are involved in response selection and reorganizing behavior for changing rewards (Shima and Tanji, 1998; Bush et al., 2002). Thus, human and experimental animal findings support a more complex organization of the cingulate gyrus than suggested by Brodmann's map.

Three lines of evidence suggest that MCC itself is comprised of two parts. First, there are two structurally unique CMAs in the cingulate sulcus with different neuronal response properties and connections. The caudal CMA (cCMA) has neurons with short latencies to muscle contractions during passive driving and projects to the same part of the striatum as primary motor cortex, while the rostral CMA (rCMA) has neurons with long-durations between discharge and contraction associated with self-paced movements and projections overlap in the striatum with those from the pre-supplementary motor area (Shima et al., 1991; Takada et al., 2001). The presence of two motor areas also suggests unique afferent circuits for their separate engagement. Second, the cingulate gyral surface has different cytologies like cortex in the sulcus and Smith (1907) and the Vogts (1919) identified anterior and posterior divisions in this region. Figure 1 shows these maps because so few perspectives beyond Brodmann's are considered in imaging research. Third, a unique class of spindle neuron occurs in the anterior but not posterior parts of MCC (Nimchinsky et al., 1995; their Fig. 3) and this supports the hypothesis of a functional dichotomy in MCC.

An important issue regarding the midcingulate region is the nature of transition between areas 24 and 23. Area 24 is agranular (i.e., lacks a layer IV), while area 23 is granular because it has this layer. If there are two MCC divisions, which one is agranular, does this transition involve a simple increase in the number of layer IV neurons, and are there unique laminar cytologies for each subarea? Although Brodmann (1909) placed the border between areas 24 and 23 at a level approximately half-way between the genu and splenium of the corpus callosum, this border may be more posterior (Vogt et al., 1995, 1997, 2003). Since Brodmann's border for areas 24 and 23 is used in functional imaging, documentation of MCC heterogeneity and posterior transitions will have a profound impact on localization research.

A striking finding of human imaging research is the consistent activation of MCC during acute noxious stimulation (Derbyshire, 2000; Peyron et al., 2000). Although noxious activation of the MCC skeletomotor region suggests a role in motor response selection, particularly as it relates to recoding of inappropriate behaviors that produce painful outcomes (Vogt et al., 1996; Davis et al., 1997), it may not explain the affective component of pain processing. Early positron emission tomography (PET) studies assessed healthy women while they self-generated sad events and activated perigenual ACC (pACC), however, middle, posterior, and retrosplenial cortices were not active (George et al. 1995, 1996). Indeed, these sites were quite distant from the MCC activity reported in the pain literature and a recent analysis of emotion showed that MCC was virtually inactive (Phan et al., 2002). In spite of these many advances,

no studies directly link pACC and MCC areas to pain and emotion functions and no joint analyses of pain and emotion have been correlated with modern morphological findings.

The present investigation evaluates structural heterogeneity within MCC, defines the transitional features of cortex between anterior and posterior cingulate cortices, and correlates these areas with activations during pain and simple emotions. The cytology of areas 24 and 23 and transitional features between them was evaluated with Nissl and immunohistochemical preparations, digital macrophotographs of each medial surface were co-registered to Talairach and Tournoux (1988) coordinates, regional borders identified, and the average position of each border from the vertical plane at the anterior commissure calculated. One functional analysis plotted noxious cutaneous thermal activations in relation to the MCC borders and a second plotted responses during simple emotions induced with scripts or facial expressions, while a control analysis identified active sites using similar stimuli that were content neutral. The joint pain and emotion analysis resolves some key questions about the unique contributions of the rCMA and cCMA and reciprocally connected gyral surface areas to behavior.

MATERIALS AND METHODS

Histological Preparations

Five brains were used that had complete cingulate gyrus staining dorsal to the corpus callosum and the characteristics for each case are provided in Table 1. All brains were obtained from the Office of the Chief Medical Examiner in cooperation with the Chief of Neuropathology in the Department of Pathology at Wake Forest University School of Medicine (Winston-Salem, NC). The brains were part of a family-approved autopsy procedure that included brain assessment prior to the present analyses. All cases were established as cognitively normal based on medical records and telephone interviews with close family members to establish the level of job and family functioning just prior to death. A neuropathological analysis, including deposition of amyloid beta peptides, neurofibrillary tangles, Lewy bodies, and neurodegeneration, confirmed that cingulate cortex was normal. A *post hoc* analysis was performed on case #6 that was cut in the horizontal plane to view borders identified in the 5 coronal cases. Two months before death case #6 had an unconscious episode, he was a heavy smoker, and there was diffuse glia in cortex. Neuronal and laminar architectures are normal in the cingulate gyrus and all thionin-stained neurons were NeuN-positive.

The medial cortex was photographed for all cases, 5 cases were cut coronally into 8-42 blocks (#1-5) and one was cut in the horizontal plane (#6), and all were re-photographed. The blocks were immersion fixed in either 10% formalin (Case 1) or 4% paraformaldehyde (Cases 2-6). Case 1 had been fixed for about 6 months and embedded in celloidin, while the latter five were fixed for 3-5 days and cryoprotected in sucrose for immunohistochemistry. Every block from all cases was sectioned into six serial series and one series each used for thionin, NeuN, SMI32, and calretinin. Sections were pretreated with 75% methanol/7.5% hydrogen peroxide, followed by a 3 min pretreatment with formic acid (NeuN only) and then a washing with distilled water and two washes in phosphate buffered saline (PBS). Sections were incubated in primary antibody in PBS (SMI32, Sternberger Monoclonals, Lutherville, MD, 1:10,000 dilution, mouse; NeuN, Chemicon, Temecula, CA, 1:1,000 dilution, mouse; calretinin, 1:3,000 dilution, mouse, Chemicon) containing 0.3% Triton X-100 and 0.5 mg/ml bovine serum albumin (BSA) overnight at 4°C. Sections were rinsed in PBS and incubated in biotinylated secondary antibody at 1:200 in PBS/Triton-X/BSA for one hour. Following rinses in PBS, sections were incubated in ABC solution (1:4; Vector) in PBS/Triton-X/BSA for one hour followed by PBS rinses and incubation in 0.05% diaminobenzidine, 0.01% H_2O_2 in a 1:10 dilution of PBS for 5 min. After PBS rinses, sections were mounted, air dried, counterstained with thionin (3 min; 0.05% in 3.7% sodium acetate, 3.5% glacial acetic acid, pH 4.5), dehydrated, and coverslipped.

Histological Data Analysis

There were four steps for the histological analysis. First, sections at a 1-2 mm interval were microscopically scanned to assess the structure of gyral areas in terms of progressive differences in cytoarchitecture and to identify centroid sections for each area. The centroid is an approximate center for an area that is used to assess cytological features; i.e., the criteria that define an area and placement of documentary microphotographs. Second, the Talairach and Tournoux coordinate system and corpus callosum of their case (1988; Figure 42) was fitted to the medial surface digital photograph of each postmortem case using two separate layers in Adobe Photoshop 6.0 software (San Jose, Ca). Each case was aligned by reducing the Talairach and Tournoux image to 50% opacity so the underlying brain could be observed. The case and coordinate system were then aligned using the anterior commissures and the body, genu and splenial borders of corpora callosi as fiducials in the z and y dimensions. Third, 2-5 microphotographs were taken from all blocks, depending on their length in the A/P plane, through layers III-VI at 150X and they were printed together for each case. Fourth, the photographs were used to guide a final assessment of where the borders of each region were located in the co-registrations so measurements from the vertical plane at the anterior commissure (VCA) could be determined and a population mean±SEM calculated.

Pain Processing

Medline searches were performed using the following key words: imaging, nociception, PET, functional magnetic resonance imaging (fMRI), pain, and noxious through 2002 in neurologically and psychiatrically healthy adults. Thirty-four relevant articles were identified that measured response using PET or fMRI during a noxious heat condition compared to none, or reduced, sensation baseline condition. References for pain and emotion analyses are provided in the online edition as “Citations for Functional Studies.” Twenty-five of the 34 articles used phasic stimuli defined as an alternating stimulus temperature or a moving stimulus lasting for <15 sec. The remaining nine articles used tonic stimuli with stationery stimuli ≥15 sec. Studies were not segregated according to standards of methodology, i.e., all studies involving noxious heat and functional imaging were entered into this review because the small number of studies available, especially for tonic heat, did not facilitate the use of methodological criteria to exclude reports. Moreover, the process of exclusion would have minimized assessment of the patterns of activity derived from the accumulated studies, which was a major aim of the current study. As it was unknown precisely where patterns would emerge, and whether or where the activation from different studies would cluster, an inclusive approach was adopted.

Emotion and Non-emotion Processing

Medline searches were performed using the following key words: PET, fMRI, cingulate, medial prefrontal, emotion, sadness, happiness, anger, fear from 1995 to 2002 in healthy adults. Studies had to employ tasks that elicited a signal in cingulate cortex ($p<0.001$ uncorrected and 0.05 corrected for multiple comparisons and z-score equivalents) in response to generating the simple primary emotions with script driven internally generated emotion or in response to pictures of emotional faces. Each selected study analyzed the data by either subtracting the signal from a basal control condition or by using an orthogonal contrast of an emotional response. Studies that failed to specify the exact emotion and/or analyzed emotion as a main effect were excluded. Selected studies used either script-driven tasks in which participants reflected on a previous and personally relevant event or relationship that elicited an emotion with validation by monitoring self-report of subjective ratings and/or physiological arousal or subjects responded to pictures of facial expressions that expressed specific emotions. It is difficult to provide “control conditions” for studies of emotion. For example, in a task requiring the subject to recall a distant and emotionally significant event, it is almost impossible to

differentiate between emotion-linked cognition from thought in the absence of emotion and memory. One way to eliminate potential biases intrinsic to studies is to analyze studies with similar sensory and cognitive parameters that lack an emotional dimension. Studies that used non-emotional, personally relevant recall of events, persons or relations, and responses to neutral faces were plotted separately as controls.

Data Extraction for Functional Analyses

All selected studies either transformed images into Talairach and Tournoux (1988) stereotactic space or normalized images to the Montreal Neurologic Institute's averaged brain. All coordinates identifying cingulate activations were included in this analysis, even when studies attributed cingulate activations to other cortical regions. Conversely, if the coordinates were described as being in cingulate cortex but they were in medial frontal areas 10, 9, 8, and/or 6, the activation was not included. The sagittal grid from the Talairach and Tournoux (1988) was co-registered to each histological case, and Case 2 and the average distance to each of the three borders was used to guide the summary plots. The different types of stimulation were color-coded and plotted onto the medial surface and, wherever possible, the positioning was checked against the original images, the authors' description, and/or ensured to be within the same or adjacent area. Inherently, there is a tendency for the images to underestimate the extent of activation because only the center of each reported region was plotted. Thus, the images may exaggerate the focal precision of activation but reflect the bias toward certain regional activations. Clustering of regional activation will be observed because studies will, on average, tend towards a central focus. This procedure has successfully been used to summarize regional activation during cognitive (Bush et al., 2000), visceral (Derbyshire, 2003), and somatic pain (Peyron et al., 2000) processing.

RESULTS

Neurocytology

An overview of the cytoarchitecture of anterior cingulate cortex for Case 2 is in Figure 2 where the arrows for layers II, III, Va, and VI in the "b" division of each section identified with brackets emphasize key structural differences. Layers Va and VI are broad but poorly differentiated in area 24b, thickest and most dense in area a24b' in anterior MCC (aMCC), and thin but quite dense in area p24b' in posterior MCC (pMCC). Layer III is progressively less neuron dense and layer II is progressively thinner in the rostrocaudal or y axis. Figure 3 compares aMCC and pMCC in NeuN and SMI32 preparations for Case 2 at higher magnification. Critical differences include the thicker layer Va with more total neurons and more NFP+ neurons in areas p24a'/b' than in areas a24a'/b'. Both posterior areas have many deep layer III NFP+ neurons that are almost undetectable in aMCC (below double arrows in Fig. 3). This is not a layer IIIc, however, because a separate layer of large pyramidal neurons cannot be detected with NeuN.

Identifying the border between area p24' and posterior cingulate cortex (PCC; area 23) requires assessment of the transition from the former agranular region and the latter granular region. This transition is characterized by an intermediate area with a dysgranular layer IV termed area 23d (d, dysgranular). Although this transition can be shown with all cases, the nature of dysgranular cortex shown in Figure 4 is for Case 1 because it was prepared with celloidin embedding and Nissl staining like cases used in classical cytoarchitectural studies. Islands of layer IV neurons are formed in area 23d as emphasized in Figure 4 with three arrows. On either side of this neuronal aggregate, the large neurons in layers IIIc and Va intermingle like they do in dysgranular areas 32 and 30. In contrast, the granular layer IV in area 23b is broad and continuous and layer Va is very dense with many small neurons as is true for area p24b'. Area p24b' also has very large neurons in layer Vb that form small clusters; two are marked with

arrows in Figure 4. Area a24b' has consistently smaller neurons in deep layer III and generally small and less dense neurons in layer V.

Cytological differentiation of areas a24' and p24' is enhanced at higher magnification and Figure 5 shows layer V in Case 3 for both parts of MCC. There are many small neurons intermingled with large pyramids in layer Va of area p24b'. The NeuN preparations (Fig. 5; p24b') show most of these small neurons have thin apical dendrites and the SMI32 preparations show that none express NFP. In contrast, many large and some moderate-sized pyramids in layers Va and Vb do express NFP. The combination of small, NFP-negative pyramids and moderate-large NFP+ pyramids in layer Va produces the high density of neurons noted for Case 2 (Figs. 2, 3). One of the outstanding features of pMCC is the very neuron dense layer Va in all cases analyzed. There are also many more large pyramids in layer Vb of area p24b' and these neurons are often NFP+. In contrast, area a24b' is comprised of moderate to large neurons throughout layer V, many of which express NFP, and layer Vb is relatively sparse with some large and NFP+ neurons. Since some cingulate cortex pyramids express calretinin (Nimchinsky et al., 1997), layer Va of MCC was explored with this antibody. Most activity was in neurons in layers I-III of pMCC and no small pyramids in this area and layer Va were calretinin-immunoreactive.

Horizontal Plane of Section

To evaluate the transition through areas p24', 23d, and 23b in single sections, case #6 was analyzed in the horizontal plane and is shown in a NeuN preparation in Figure 6. Interpretation of this figure is best started with the architecture of area 31 because it has a very thick layer IV and the relative size and density of large pyramidal neurons emphasizes those in layer IIIc over layer Va. Area 23b, in contrast, has a layer Va comprised of both large and many small pyramids that is very dense as noted above, a layer IV that is thinner than in area 31, and the largest pyramids in layer IIIc about equal in size to those in layer Va. The composition of area p24a' in this case is as already described with a dense layer Va and a deep layer III that has diffuse and moderate-sized pyramids.

To demonstrate area 23d in case #6, 3 photographs were taken to bracket a large aggregate of layer IV neurons and demonstrate the dysgranular nature of this area. In the center picture ("23d, 2"), there is a clearly identifiable layer IV, while on each adjacent photograph, layer IV disappears at the level of the double asterisks and large neurons in layers IIIc, and Va intermingle. The nature of a dysgranular cortex with a variable-thickness layer IV, therefore, can be demonstrated in both planes of section.

Standardized Borders

The digital medial surface photograph of each case was co-registered to the Talairach and Tournoux (1988) coordinate system and corpus callosum and shown in Figure 7A. Once a case was co-registered, borders were identified in histological sections and a distance calculated from the VCA to each border for each case. Table 2 provides these distances and the mean ±SEM for all cases.

Pain Processing

Thirty-eight articles reported 69 cingulate activations during noxious thermal cutaneous stimulation. All sites were plotted onto the Case 2 medial surface after co-registration of the atlas coordinates and location of the three MCC borders. Eighty-four percent of cingulate activations were in MCC, while others were in either PCC or pACC (Fig. 7B). Of the 58 MCC sites in MCC, 26 were in aMCC and 32 were in pMCC. Since long-duration noxious stimuli could be associated with affective responses like unpleasantness, the activations in Figure 7B were coded for short (<15 sec; red) or long (≥15 sec; blue) durations. Of the 32 sites associated

with short stimulation, 18 (56%) were in pMCC, while 14 (44%) were in aMCC. The non-homogeneous distribution of sites in pMCC was amplified by aggregation of activations around the VAC and a double arrow in Figure 7B emphasizes that only 5 short-duration sites were in the posterior ⅔ of pMCC, while 13 aggregated at the VAC. There were 13 long-duration sites in both aMCC and pMCC. In pMCC, 5 were in the posterior ⅔ and 8 in anterior ⅓, rostral to double arrow. Although the total number of activations was about the same in both divisions of MCC, aggregation of short-duration sites around the VCA in pMCC emphasizes a topographic specialization within pMCC not present in aMCC.

Emotion and Non-emotion Processing

Studies of simple emotions were selected that monitored recognition, recall, and retrieval of emotional material with personally relevant scripts of person and/or events or emotionally induced, non-personally relevant facial expressions. Figure 7C shows 45 total emotion activations in cingulate cortex; 10 were to fearful faces and 6 of these were in aMCC, one in pMCC, two in PCC, and one in pACC. Anger evoked diffuse activity with two sites each in pACC, pMCC, and aPCC. Sites activated by sadness or happiness were almost completely separated from those for fear and anger. Sadness activated the ventral portion of the pACC, mainly areas 24a and 25 and happiness activated the two extreme parts of cingulate cortex; 10 sites were in pACC, rostral to most of the “sad” sites, and 7 sites were in pPCC.

Critical to assessing the extent of a specific role of aMCC in fear is the assurance that it is not also activated during non-emotional conditions indicating a wider role in brain function. Personally relevant memory that did not involve emotion consistently activated areas 23 and 31 in ventral PCC (vPCC; Fig. 7D). These included most activations to neutral faces. Only two sites were in pACC and 3 were in pMCC. Thus, vPCC activations during emotion are associated with a general role in facial recognition and/or visuospatial or personal orientation, rather than regulation of emotion *per se*. In contrast, fear activity in aMCC is specifically related to emotion and not other parameters of facial or verbal recognition as was also true for sadness and happiness in pACC.

DISCUSSION

The structure of MCC has been defined in terms of the unique cytological characteristics for its anterior and posterior parts. All cases had a very neuron dense layer Va in pMCC and PCC and a dysgranular area 23d between pMCC and PCC. These differences were in tissue processed according to classical methods and current immunohistochemical procedures in two planes of section and the Brodmann map requires significant alterations to bring it in line with this cytological organization. Furthermore, the analysis of nociceptive activations provides a striking confirmation that MCC is a major location of pain processing events, although heterogeneities in the topography of pMCC activation sites distinguish it from aMCC. Nociceptive activation emphasizes the role of MCC in response selection and such activity in aMCC is enhanced by fear and contributes to its vulnerability in chronic pain syndromes.

Neuroanatomical Organization

The most striking finding of this survey of midcingulate histology is the presence of a layer Va that is dense with both small and large pyramids in areas p24’ and 23. Layer IV has many small neurons, however, these have mainly intracortical connections (Peters and Jones, 1984) and, until the present analysis, we viewed the granularity of area 23 as typically defined by layer IV (Vogt et al., 1987, 1997). Although area 23 does have a granular layer IV, a prominent part of its parvicellular features are due to the composition of layer Va associated with small pyramidal neurons. In fact, at low magnification, the most prominent layer in area 23 is layer Va, not layer IV (Vogt et al., 2001a). The concept of a layer Va with small and

densely packed pyramids resolves another issue; localization of the area 24/23 border in MCC. The presence of many small pyramids in layer Va, dysgranular aggregates in layer IV, or as a separate layer IV provide intermediate levels of transition between agranular and granular cortices and variable processing circuits between afferent inputs from the thalamus and efferent projections to motor systems and other cortices. The specific roles of each laminar placement and function of small pyramids in this context are not known.

The nature of transition from agranular area 24 to granular area 23 can be stated for the first time in primates and it improves understanding of area 23 and MCC. In addition to the high density of small pyramids in layer Va, there is an intermediate dysgranular layer IV in area 23d. The concept of a dysgranular cortex has been thoroughly discussed for cingulate (Vogt et al., 1997, 2001b, 2003), insular (Mufson et al., 1997), and orbitofrontal (Hof et al., 1995) cortices. In cingulate cortex, however, this has been discussed only for area 32' as it relates to cingulofrontal transition and for area 30 in relation to differentiation of granular retrosplenial area 29 and isocortical area 23a (Vogt, 1976; Vogt et al., 2003). Cortical transition along the cingulate gyral surface involves a high density of small neurons in layer Va in pMCC, formation of dysgranular aggregates of neurons in layer IV of area 23d, and a fully granular layer IV and very dense layer Va in areas 23a-c. Thus, a significant revision is required for the Brodmann map that is generally available for functional imaging because the concept of only two cingulate regions (i.e., ACC and PCC) is not tenable because they do *not* represent uniform structural or functional entities.

Emotion and Pain Processing

Cingulate cortex is one of the most frequently activated regions during acute pain (Derbyshire, 2000; Peyron et al., 2000) and the current functional analyses confirmed the pivotal role of MCC. As the complexity of cingulate cytology and connections is uncovered, these issues need reconsideration in the context of the many studies of emotion performed over the past decade. Most acute nociceptive activations were around the VCA in pMCC and throughout aMCC. Since the juncture of aMCC and pMCC has enhanced activation during hypnosis when the intensity and unpleasantness of noxious stimuli is increased (Faymonville et al., 2000), it was not surprising to see the high density of activations around the VCA. We expected that long-duration noxious stimulation would increase affect and activity in aMCC because of the high level of fear activations in this region, however, this hypothesis was rejected because long-duration stimuli evoked activity that was evenly distributed in MCC. Since aMCC has also been activated during anxiety related to aversive conditional stimuli (Buchel et al., 1998, 1999) and pain anticipation (Chua et al., 1999; Hsieh et al., 1999; Sawamoto et al., 2000; Porro et al., 2002), it appears that noxious activation in aMCC is associated with fear and anxiety that are critical to avoidance behaviors driven by the rCMA. A specific circuit for these interactions is suggested below.

Although the pain analysis showed that the posterior ⅔ of pMCC had few pain sites, Bentley et al. (2003) observed a very early (400-540 msec latency), laser-evoked, positive potential in the posterior part of pMCC. Since this part of pMCC receives input from the limitans nucleus of thalamus, which itself receives spinothalamic inputs (Vogt et al., 1987; Vogt et al., 1993), it seems paradoxical it is least activated in functional imaging studies. The short latency of the P2 response may be outside the resolution of current imaging methods and the posterior pMCC may be involved in very early orienting responses to noxious stimuli through the cCMA (Matelli et al., 1991; Zilles et al., 1995) and its spinal cord and motor cortex projections (Dum and Strick, 1993; Morecraft and Van Hoesen, 1998). Therefore, the very early, P2 evoked potential may constitute a third contribution of cingulate cortex to pain processing: a) pMCC coordinates the earliest skeletomotor reflex responses through the cCMA, b) aMCC coordinates fear and avoidance with skeletomotor activity through the rCMA, and c) pACC

regulates affect in relation to autonomic functions (Porro et al., 2003). It should also be noted that neurons in the cCMA are more active during cue-triggered movements than during self-paced movements and there is a longer pre-movement delay in the anterior than posterior parts of cingulate sulcal cortex (Shima et al., 1991). These physiological differences of the rostral and caudal CMAs support differential processing circuits within MCC. These observations also suggest a progression in cingulate engagement by noxious stimuli beginning in pMCC, proceeding to aMCC, and ending in pACC to accommodate a progressively larger and longer duration painful "burden" and coordinated skeletomotor and autonomic processing.

Functional MCC Circuits

The role of MCC in skeletomotor regulation and response selection is well known (Devinsky et al., 1995), however, this does not address the reasons for two cingulate motor areas and the dichotomy in MCC organization. This question can be addressed from the perspective of two intrinsic circuits in aMCC and pMCC. The aMCC circuit is shown in Figure 8 which begins with two monkeys in which Fast Blue was injected into the rCMA (A.) to retrogradely label inputs to this region from the cingulate gyrus and tritiated amino acids (B.) to anterogradely label terminals from this area (Van Hoesen et al., 1993). These cases demonstrate dense and reciprocal connections between the gyral surface and rCMA and emphasize that inputs to rCMA are more widespread than are reciprocal, but not equivalent, connections. The aMCC diagram (C.) suggests that fear, associated memories, and cognitive schemata are stored in aMCC. Activation of the circuit by nociceptive inputs from the thalamus induces fear and memories of similar events and triggers outcome prediction. This activity drives the rCMA to enhance avoidance responses via layer V projections to motor structures. It may also change behaviors based on new outcomes and changes in the reward properties of particular behaviors (Shima and Tanji, 1998; Bush et al., 2002).

Why is a second circuit needed in pMCC? A pMCC circuit is not driven by any emotion and it is poorly engaged, though not inactive, by noxious stimulation and it may receive less input from thalamic nuclei that receive spinothalamic and spinoreticular inputs. Activity in the cCMA tends to be more closely linked temporally to motor output (i.e., shorter latency between neuronal discharge and muscle contractions; Shima et al., 1991), projects to a part of the striatum that also receives primary motor input (Takada et al., 2001), and may be involved in the earliest sensorimotor orienting and reflex responses (Bentley et al., 2003) rather than complex behaviors involving assessment of outcomes. Finally, pMCC and dorsal PCC have profound inputs from inferior parietal cortex that are much less prominent to aMCC (Vogt and Pandya, 1987) and this may contribute to orientation in space and spatial guiding of behavior.

Differential Vulnerability of aMCC & pMCC in Chronic Pain Syndromes

The ultimate test of any neurobiological model of structure/function associations is the extent to which cortical units are selectively vulnerable to neuronal diseases. Studies of chronic pain syndromes suggest that the two divisions of MCC are differentially impacted by chronic somatic (pMCC) and visceral (aMCC) pain. Hsieh et al. (1995) reported activity of right pMCC during ongoing neuralgia pain. This activation was revealed by comparing activity during the painful state with a lidocaine-nerve-block, pain-alleviated state. The neuropathic response was caudal to acute tonic activity observed here in the posterior ⅔ of pMCC. Derbyshire et al. (2002) reported increased cerebral blood flow in pMCC during phasic pain stimulation in patients with low back pain close to pMCC that was also more active in patients with atypical facial pain (Derbyshire et al., 1994). A recent report of relief of trigeminal pain using electrostimulation revealed correlates of pain relief in pMCC (Willoch et al., 2003). Thus, chronic pain with a somatic etiology critically involves pMCC and may selectively disrupt early orientation responses.

In contrast, noxious visceral stimulation in patients with chronic visceral pain associated with irritable bowel syndrome (IBS) activate aMCC (Mertz et al., 2000; Naliboff et al., 2001) and activity in pMCC in IBS is rare (Derbyshire, 2003). These data make a case for selective vulnerability of aMCC in IBS. Indeed, IBS is associated with numerous psychosocial stress factors including depression, distress, rape, and/or physical abuse (Leserman et al., 1996; Drossman et al., 2000) and these factors could enhance fear and engage the same region activated during fear. Impaired anticipatory actions associated with IBS during visceral stimulation show a prominent role of aMCC and the circuit above emphasizes the role of aMCC in cognitive schemata disordered in IBS. The enhanced vulnerability of aMCC to chronic visceral pain appears to be due to the fact that aMCC uses the nociceptive signal and fear to modulate avoidance behaviors. Finally, a case of IBS with a history of physical and sexual abuse not only demonstrated enhanced activation of aMCC during noxious rectal distension, but this response and persistent visceral pain resolved following cognitive-behavioral therapy and termination of marriage to an abusive spouse (Drossman et al., 2003). This case emphasizes the importance of aMCC to chronic visceral pain syndromes, and although pMCC may also be impacted, targeting cognitive therapies to aMCC must be part of the long-term goal of objective assessment of treatment outcomes with imaging modalities.

Acknowledgements

We greatly appreciate the comments of Dr. George Bush on an early version of this manuscript. This work was supported by NIH/NINDS grants #NS38485 and #NS44222 (BAV) and the Pittsburgh Foundation and the John F. and Nancy A. Emmerling Fund (SWGD).

References

Bentley DE, Derbyshire SWG, Youell PD, Jones AKP. Caudal cingulate cortex involvement in pain processing: an inter-individual laser evoked potential source localization study using realistic head models. Pain 2003;102:265–271. [PubMed: 12670668]

Braak H. A primitive gigantopyramidal field buried in the depth of the cingulate sulcus of the human brain. Brain Res 1976;109:219–233. [PubMed: 1276913]

Braak, H. Architectonics of the Human Telencephalic Cortex. Berlin: Springer-Verlag; 1980.

Brodmann, K. Vergleichende Lokalisationslehre der Grosshirnrinde in ihren Prinzipien dargestellt auf Grund des Zellenbaues. Barth; Leipzig: 1909.

Buchel C, Dolan RJ, Armony JL, Fiston KJ. Amygdala-hippocampal involvement in human aversive trace conditioning revealed through event-related functional magnetic resonance imaging. J Neurosci 1999;19:10869–76. [PubMed: 10594068]

Buchel C, Morris J, Dolan RJ, Friston KJ. Brain systems mediating aversive conditioning: an event-related fMRI study. Neuron 1998;20:947–57. [PubMed: 9620699]

Bush G, Luu P, Posner MI. Cognitive and emotional influences in anterior cingulate cortex. Trends Cog Sci 2000;4:215–222.

Bush G, Vogt BA, Holmes J, Dale AM, Greve D, Jenike MA, Rosen BR. Dorsal anterior cingulate cortex: A role in reward-based decision-making. Proc Natl Acad Sci 2002;99:523–528. [PubMed: 11756669]

Chua P, Krams M, Toni I, Passingham R, Dolan R. A functional anatomy of anticipatory anxiety. NeuroImage 1999;9:563–71. [PubMed: 10334900]

Davis KD, Taylor SJ, Crawley AP, Wood ML, Mikluis DJ. Functional MRI of pain- and attention-related activations in the human cingulate cortex. J Neurophysiol 1997;77:3370–3380. [PubMed: 9212281]

Derbyshire SWG. Exploring the pain “neuromatrix”. Curr Rev Pain 2000;6:467–477. [PubMed: 11060593]

Derbyshire SWG. Meta analysis of neuroimaging data reveals differential activation from upper and lower gastrointestinal distension. Am J Gastroenterol. 2003in press

Derbyshire SWG, Jones AKJ, Creed F, Starz T, Meltzer CC, Townsend DW, Peterson AM, Firestone L. Cerebral responses to noxious thermal stimulation in chronic low back apin patients and normal controls. NeuroImage 2002;16:158–168. [PubMed: 11969326]

Derbyshire SWG, Jones AKP, Devani P, Friston KJ, Feinmann C, Harris M, Pearce S, Watson JD, Frackowiak RSJ. Cerebral responses to pain in patients with atypical facial pain measured by positron emission tomography. J Neurol Neurosurg Psychiatry 1994;57:1166–1172. [PubMed: 7931375]

Devinsky O, Morrell MJ, Vogt BA. Contributions of anterior cingulate cortex to behavior. Brain 1995;118:279–306. [PubMed: 7895011]

Drossman DA, Ringel Y, Vogt BA, Leserman J, Lin W, Smith JK, Whitehead W. Alterations of brain activity associated with resolution of emotional distress and pain in a case of severe irritable bowel syndrome. Gastroenterology 2003;124:754–761. [PubMed: 12612913]

Drossman DA, Whitehead WE, Toner BB, Diamant N, Hu YJB, Bangdiwala SI, Jia H. What determines severity among patients with painful functional bowel disorders? Am J Gastroenterol 2000;95:974–980. [PubMed: 10763947]

Dum, RP.; Strick, PL. Cingulate motor areas. In: Vogt, BA.; Gabriel, M., editors. Neurobiology of Cingulate Cortex and Limbic Thalamus. Birkhäuser; Boston: 1993. p. 415-441.

Elliot R, Friston KJ, Dolan RJ. Dissociable neural responses in human reward systems. J Neurosci 2000;20:6159–65. [PubMed: 10934265]

Faymonville ME, Laureys S, Degueldre C, Del Fiore G, Luxen A, Franck G, Lamy M, Maquet P. Neural mechanisms of antinociceptive effects of hypnosis. Anesthesiology 2000;92:1257–1267. [PubMed: 10781270]

Fischer H, Andersson JL, Furmark T, Fredrickson M. Fear conditioning and brain activity: a positron emission tomography study in humans. Behav Neurosci 2000;114:671–80. [PubMed: 10959525]

George MS, Ketter TA, Parekh PI, Horwitz B, Herscovitch P, Post RM. Brain activity during transient sadness and happiness in healthy women. Amer J Psychiatry 1995;152:341–351. [PubMed: 7864258]

George MS, Ketter TA, Parekh PI, Herscovitch P, Post RM. Gender differences in regional cerebral blood flow during transient self-induced sadness or happiness. Biolog Psychiatry 1996;40:859–871.

Grefkes C, Geyer S, Schormann T, Roland P, Zilles K. Human somatosensory area 2: observer-independent cytoarchitectonic mapping, interindividual variability, and population map. NeuroImage 2001;14:617–631. [PubMed: 11506535]

Hof PR, Mufson EJ, Morrison JH. Human orbitofrontal cortex cytoarchitecture and quantitative immunohistochemical parcellation. J Comp Neurol 1995;359:48–68. [PubMed: 8557847]

Hsieh JC, Stone-Elander S, Ingvar M. Anticipatory coping of pain expressed in the human anterior cingulate cortex: a positron emission tomography study. Neurosci Lett 1999;262:61–4. [PubMed: 10076873]

Lane RD, Reiman GL, Ahern GE, Schwartz GE, Davidson RJ. Neuroanatomical correlates of happiness, sadness, and disgust. Amer J Psychiatry 1997;154:926–33. [PubMed: 9210742]

Leserman J, Drossman DA, Li Z, Toomy TC, Nachman G, Glogau L. Sexual and physical abuse history in gastroenterology practice: How types of abuse impact health status. Psychosomatic Med 1996;58:4–15.

Luppino G, Matelli M, Camarda RM, Gallese V, Rizzolatti G. Multiple representations of body movements in mesial area 6 and the adjacent cingulate cortex: An intracortical microstimulation study in the macaque monkey. J Comp Neurol 1991;311:463–482. [PubMed: 1757598]

Matelli M, Luppino G, Rizzolatti G. Architecture of superior and mesial Area 6 and the adjacent cingulate cortex in the macaque monkey. J Comp Neurol 1991;311:445–462. [PubMed: 1757597]

Mertz H, Morgan V, Tanner G, Pickens D, Price R, Shyr Y, Kessler R. Regional cerebral activation in irritable bowel syndrome and control subjects with painful and nonpainful rectal distension. Gastroenterology 2000;118:842–848. [PubMed: 10784583]

Morecraft RJ, Van Hoesen GW. Cingulate input to the primary and supplementary motor cortices in the rhesus monkey: Evidence for somatotopy in Areas 24c and 23c. J Comp Neurol 1992;322:471–489. [PubMed: 1383283]

Morecraft RJ, Van Hoesen G. Convergence of limbic input to the cingulate motor cortex in the rhesus monkey. Brain Res Bull 1998;45:209–232. [PubMed: 9443842]

Mufson, EJ.; Sobreviela, T.; Kordoer, JH. Chemical neuroanatomy of the primate insula cortex: relationship to cytoarchitectonics, connectivity, function, and neurodegeneration. In: Bloom, FE.; Björklund, A.; Hökfelt, T., editors. Handbook of Chemical Neuroanatomy; The Primate Nervous System. 13. 1997. p. 377-454.

Nimchinsky EA, Vogt BA, Morrison JH, Hof PR. Spindle neurons of the human anterior cingulate cortex. J Comp Neurol 1995;355:27–37. [PubMed: 7636011]

Nimchinsky EA, Vogt BA, Morrison JH, Hof PR. Neurofilament and calcium-binding proteins in the human cingulate cortex. J Comp Neurol 1997;384:597–620. [PubMed: 9259492]

Naliboff BD, Derbyshire SWG, Munakata J, Berman S, Mandelkern M, Chang L, Mayer EA. Cerebral activation in patients with irritable bowel syndrome and control subjects during rectosigmoid stimulation. Psychosom Med 2001;63:365–375. [PubMed: 11382264]

Peters, A.; Jones, EG. Cerebral Cortex. 4. Plenum Press; NY: 1984.

Peyron R, Laurent B, Garcia-Larrea L. Functional imaging of brain responses to pain. A review and meta-analysis. Neurophysiol Clin 2000;30:263–288. [PubMed: 11126640]

Phan KL, Wager T, Taylor SF, Liberzon I. Functional neuroanatomy of emotion: A meta-analysis of emotion activation studies in PET and fMRI. NeuroImage 2002;16:331–348. [PubMed: 12030820]

Porro CA, Baraldi P, Pagnoni G, Serafinin M, Facchin P, Maieron M, Nichelli P. Does anticipation of pain affect cortical nociceptive circuits? J Neurosci 2002;22:3206–3214. [PubMed: 11943821]

Porro CA, Cettolo V, Francescato MP, Baraldi P. Functional activity mapping of the mesial hemispheric wall during anticipation of pain. NeuroImage 2003;19:1738–1747. [PubMed: 12948728]

Roland PE, Zilles K. Functions and structures of the motor cortices in humans. Curr Opinion Neurobiol 1996;6:773–781.

Sawamoto N, Honda M, Okada T, Hanakawa T, Kanda M, Fukuyama H, Konishi J, Shibasaki H. Expectation of pain enhances responses to nonpainful somatosensory stimulation in the anterior cingulate cortex and parietal operculum/posterior insula: an event-related functional magnetic resonance imaging study. J Neurosci 2000;20:7438–45. [PubMed: 11007903]

Shima K, Aya K, Mushiake H, Inase M, Aizawa H, Tanji J. Two movement-related foci in the primate cingulate cortex observed in signal-triggered and self-paced forelimb movements. J Neurophysiol 1991;65:188–202. [PubMed: 2016637]

Shima K, Tanji J. Role for cingulate motor area cells in voluntary movement selection based on reward. Science 1998;282:1335–1338. [PubMed: 9812901]

Simpson JR Jr, Drevets WC, Snyder AZ, Gusnard DA, Raichle ME. Emotion-induced changes in human medial prefrontal cortex: II. During anticipatory anxiety. Proc Natl Acad Sci USA 2001;98:688–693. [PubMed: 11209066]

Smith GE. A new topographical survey of the human cerebral cortex, being an account of the distribution of the anatomically distinct cortical areas and their relationship to the cerebral sulci. J Anat 1907;41:237–254.

Takada M, Tokuno H, Hamada I, Inase M, Ito Y, Imanishi M, Hasegawa N, Akazawa T, Hatanaka N, Nambu A. Organization of inputs from cingulate motor areas to basal ganglia in macaque monkey. Eur J Neurosci 2001;14:1633–1650. [PubMed: 11860458]

Talairach, J.; Tournoux, P. Co-Planar Stereotaxic Atlas of the Human Brain. New York: Thieme Medical Publishers, Inc; 1988.

Van Hoesen, GW.; Morecraft, RJ.; Vogt, BA. Connections of the monkey cingulate cortex. In: Vogt, BA.; Gabriel, M., editors. Neurobiology of Cingulate Cortex and Limbic Thalamus. Birkhäuser; Boston: 1993. p. 249-284.

Vogt BA. Retrosplenial cortex in the rhesus monkey: A cytoarchitectonic and Golgi study. J Camp Neuro1 1976;169:63–98.

Vogt, BA. Structural organization of cingulate cortex: Areas, neurons, and somatodendritic transmitter receptors. In: Vogt, BA.; Gabriel, M., editors. Neurobiology of Cingulate Cortex and Limbic Thalamus. Birkhäuser; Boston: 1993. p. 19-70.

Vogt BA, Derbyshire SWG, Jones AKP. Pain processing in four regions of human cingulate cortex localized with coregistered PET and MR imaging. Eur J Neurosci 1996;8:1461–1473. [PubMed: 8758953]

Vogt, BA.; Hof, PR.; Vogt, LJ. Cingulate Gyrus. In: Paxinos, G.; Mai, JK., editors. The Human Nervous System. second edition. Academic Press; 2003. in press

Vogt BA, Nimchinsky EA, Vogt LJ, Hof PR. Human cingulate cortex: Surface features, flat maps, and cytoarchitecture. J Comp Neurol 1995;359:490–506. [PubMed: 7499543]

Vogt BA, Pandya DN. Cingulate cortex of the rhesus monkey: II. Cortical afferents. J Comp Neurol 1987;262:271–289. [PubMed: 3624555]

Vogt BA, Rosene DL, Pandya DN. Cingulate cortex of the rhesus monkey: I. Cytoarchitecture and thalamic afferents. J Comp Neurol 1987;262:256–270. [PubMed: 3624554]

Vogt, BA.; Vogt, LJ.; Hof, PR. Patterns of cortical neurodegeneration in Alzheimer's disease: Subgroups, subtypes, and implications for staging strategies. In: Hof, PR.; Mobbs, CV., editors. Functional Neurobiology of Aging. Academic Press; NY: 2001a. p. 111-129.

Vogt, BA.; Vogt, LJ.; Nimchinsky, EA.; Hof, PR. Primate cingulate cortex chemoarchitecture and its disruption in Alzheimer's disease. In: Bloom, FE.; Björklund, A.; Hökfelt, T., editors. Handbook of Chemical Neuroanatomy, The Primate Nervous System. 13. Elsevier; Amsterdam: 1997. p. 455-528.

Vogt BA, Vogt LJ, Perl DP, Hof PR. Cytology of human caudomedial cingulate, retrosplenial, and caudal parahippocampal cortices. J Comp Neurol 2001b;438:353–376. [PubMed: 11550177]

Vogt C, Vogt O. Allgemeinere Ergebnisse unserer Hirnforschung. J Psychol Neurol 1919;25:279–461.

Willoch F, Gamringer U, Medele R, Steude U, Tölle TR. Analgesia by electostimulation of the trigeminal ganglion in patients with trigeminopathic pain: a PET activation study. Pain 2003;103:119–130. [PubMed: 12749966]

Zilles K, Schlaug G, Matelli M, Luppino G, Schleicher A, Qü M, Dabringhaus A, Seitz R, Roland PE. Mapping of human and macaque sensorimotor areas by integrating architecture, transmitter receptor, MRI and PET data. J Anat 1995;187:515–537. [PubMed: 8586553]

ABBREVIATIONS

a, A
: anterior

aMCC
: anterior midcingulate corte

b
: body of corpus callosum

BSA
: bovine serum albumin

cgs
: cingulate sulcus

CMA (r/c)
: cingulate motor areas; rostral/caudal

fMRI
: functional magnetic resonance imaging

g
: genu of corpus callosum

IBS
: irritable bowel syndrome

ICC
: intracortical circuit

MCC
: midcingulate cortex

NeuN
: neuron-specific nuclear binding protein

NFP
intermediate neurofilament proteins

p, P
posterior

pACC
perigenual anterior cingulate cortex

PBS
phosphate buffered saline

PCC
posterior cingulate cortex

PET
positron emission tomography

pMCC
posterior midcingulate cortex

RSC
retrosplenial cortex

s
splenium of corpus callosum

spls
splenial sulcus

VCA
vertical plane at the anterior commissure

vPCC
ventral posterior cingulate cortex

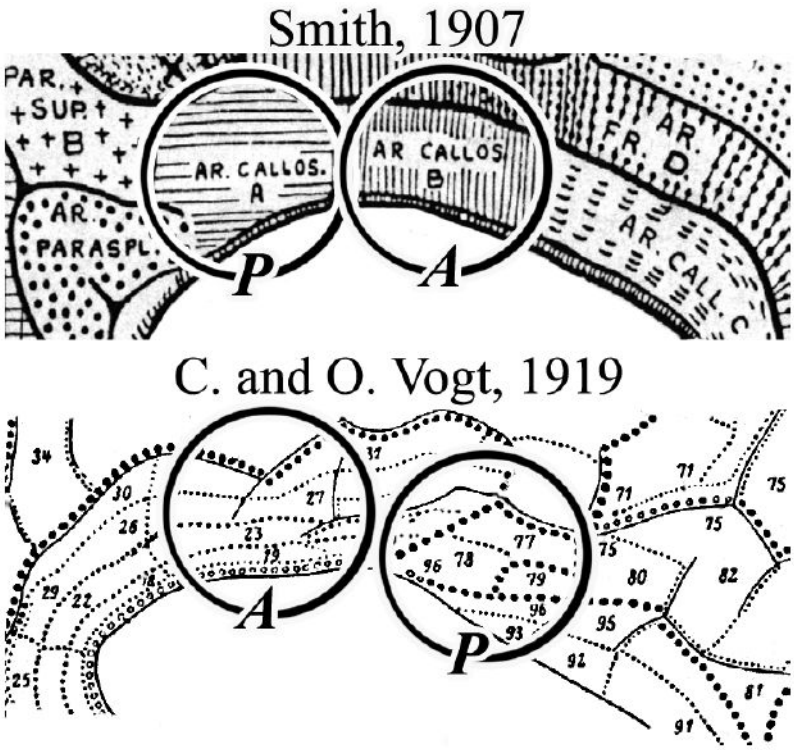

Figure 1.

Two maps of cingulate cortex showing multiple rostrocaudal subdivisions (from Braak, 1980) rather than only anterior and posterior divisions reported by Brodmann. These maps raise questions about transitional cortex between Brodmann's areas 23 and 24 and cytological variations in the dorsoventral orientation. A, anterior and P, posterior divisions of recently defined MCC.

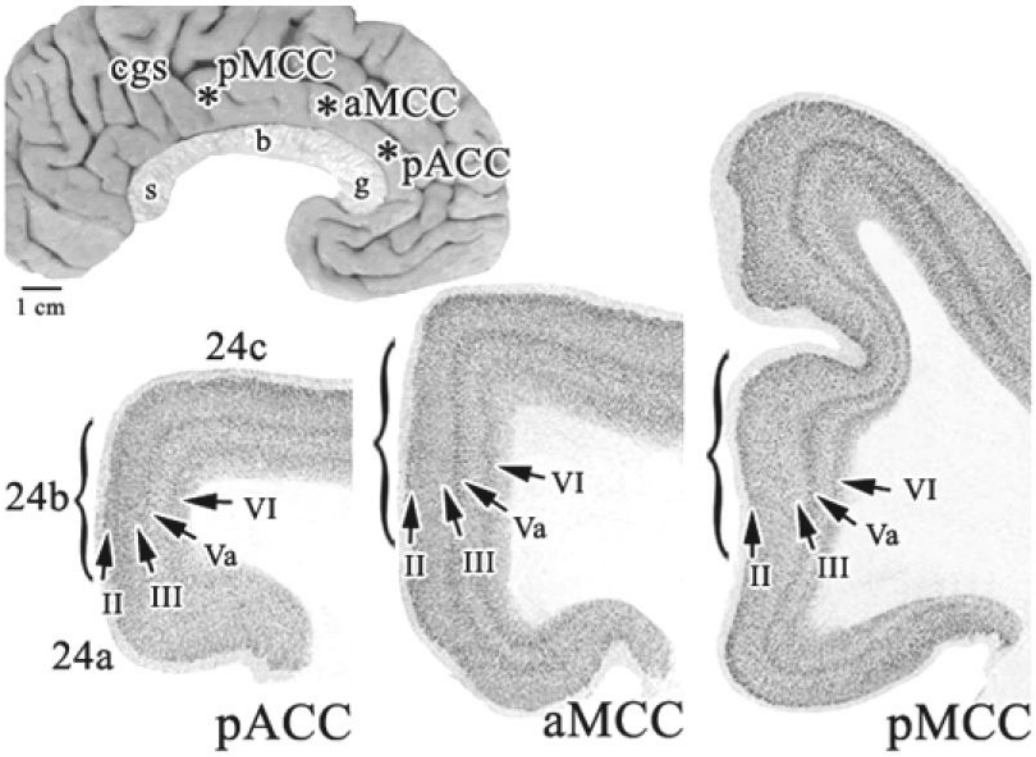

Figure 2.

Overview of areas forming the anterior cingulate region dorsal to the corpus callosum in Case 2. The coronal sections were photographed at the asterisks on the medial surface. Each arrow points to a layer in each "b" division which are marked with parentheses. Profound changes in laminar thickness and neuron density are apparent. cgs, cingulate sulcus; g, genu; b, body; s, splenium of the corpus callosum.

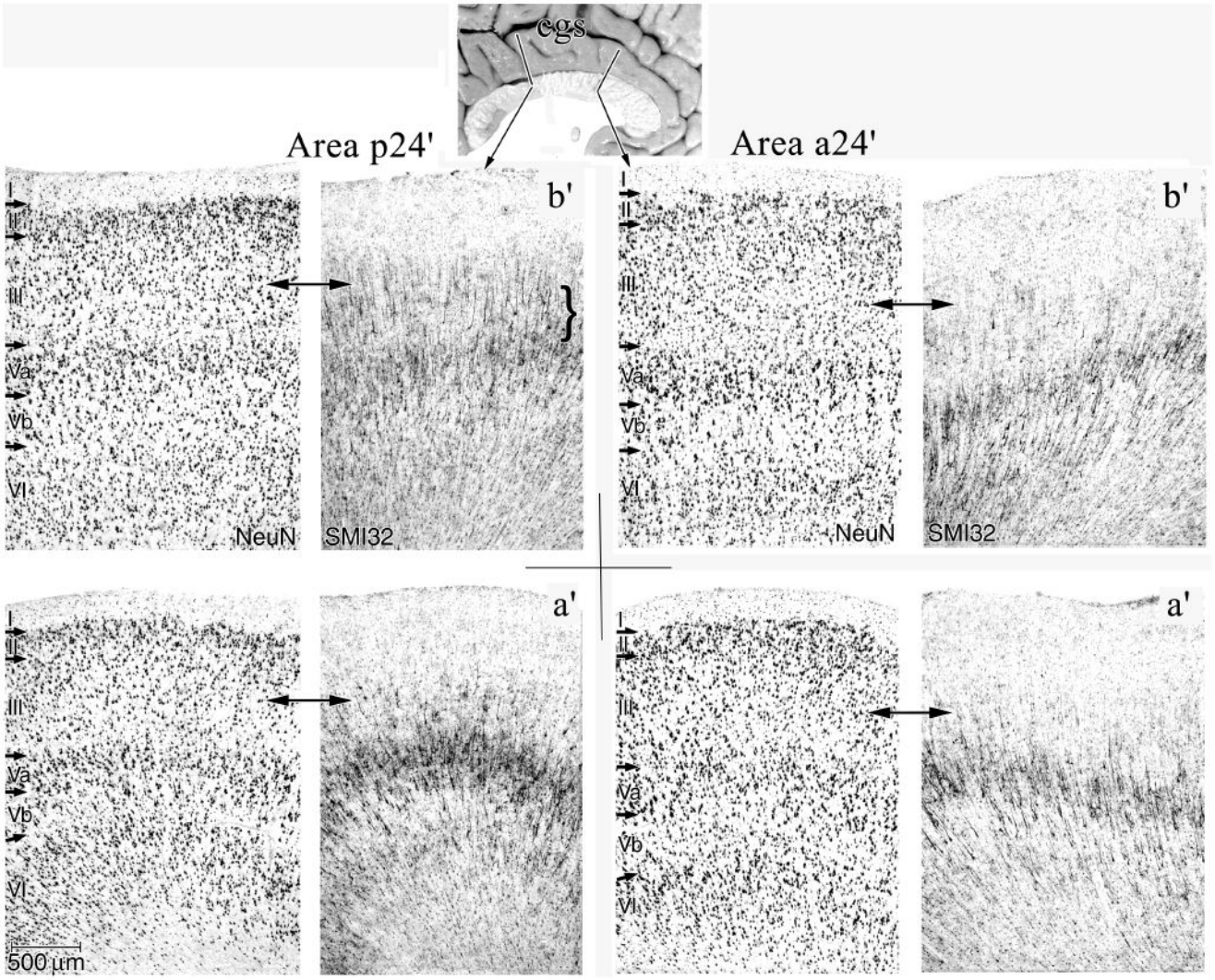

Figure 3.

Features of MCC areas a24' and p24' for both "a" and "b" subdivisions in NeuN and SMI32 of Case 2. Of particular note are the higher densities of NFP-expressing neurons in deep layer III (SMI32; below double arrows) and the greater density of neurons in layer Va and their expression of NFP in area p24'. Since the layers in NeuN and SMI32 sections were exactly co-registered, they are not relabeled in SMI32.

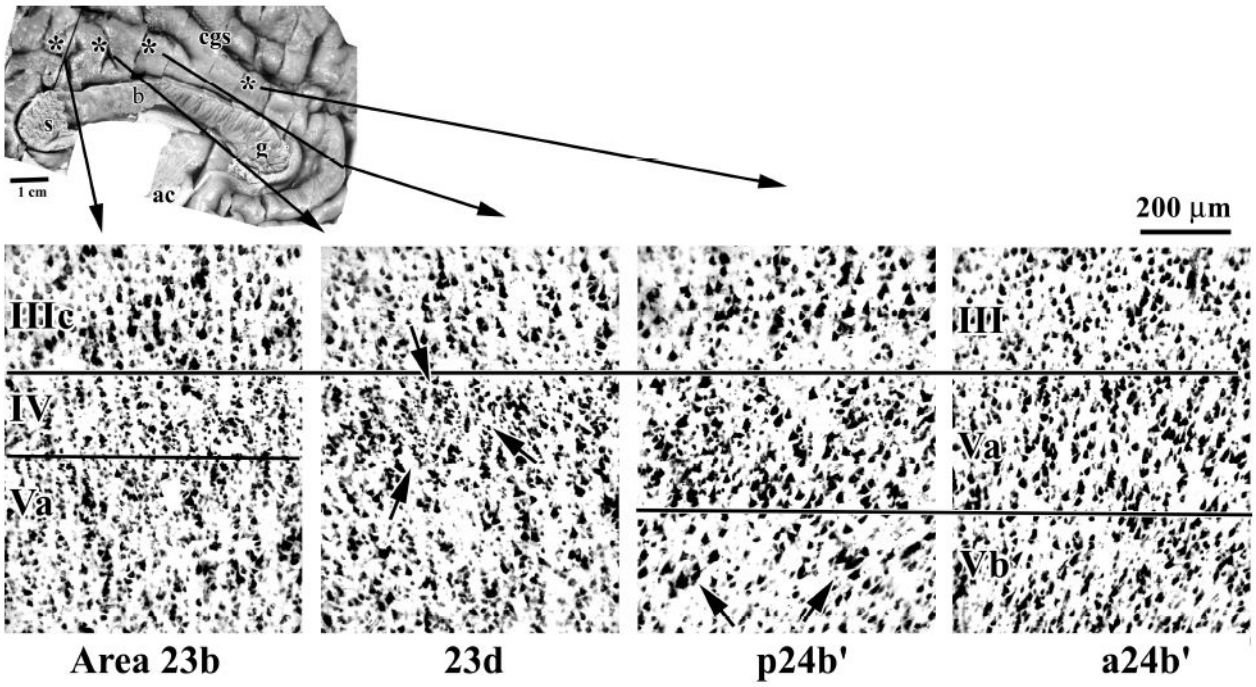

Figure 4.

The border between areas p24’ and 23 includes a transition from the agranular anterior to granular posterior cortices as shown here with thionin-stained Case 1. Area 23b has a continuous granular layer IV, while area 23d has a dysgranular layer IV that forms clumps or islands of neurons between layers IIIc and Va; one island is identified with three arrows. Area 23 also has a very dense layer Va with many small pyramids as does area p24b’. Area p24b’ has very large neurons in layer Vb that form small aggregates; two of which are marked with arrows. Area a24b’ has consistently smaller neurons in deep layer III and generally small and less dense neurons in layer V.

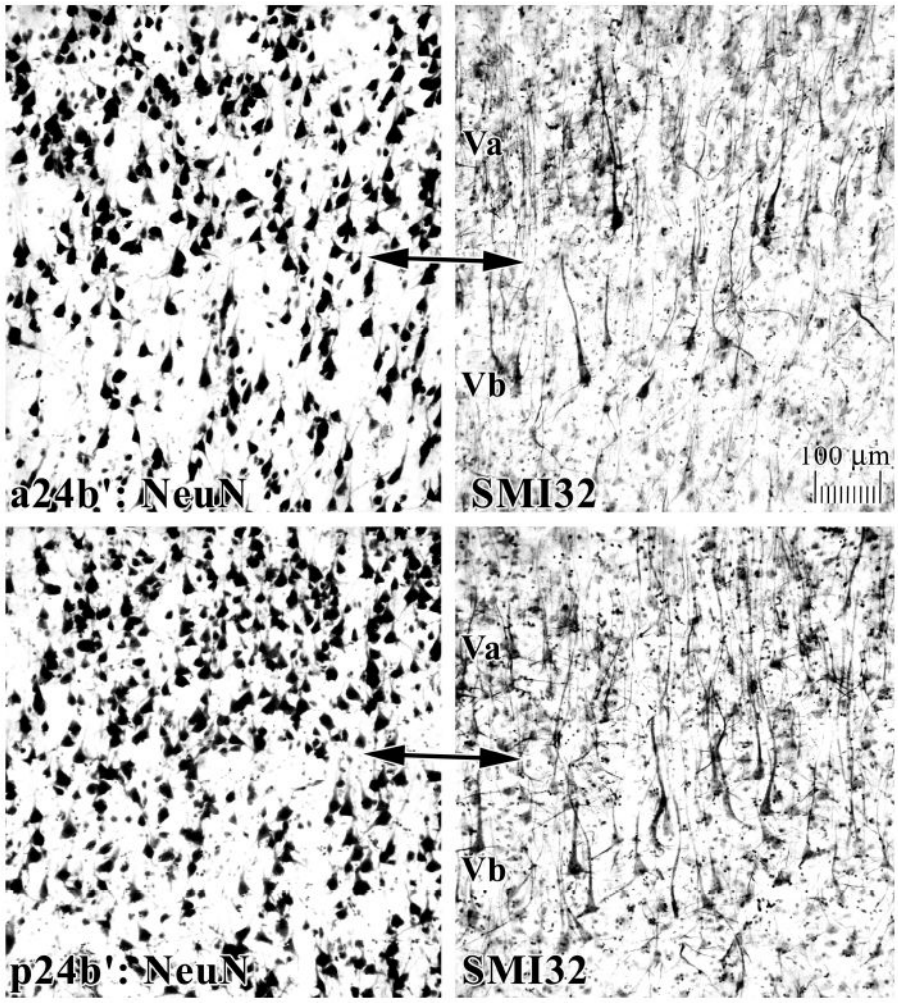

Figure 5.
Layer V differentiation is pivotal to transition in MCC, defining aMCC and pMCC, and it is magnified here for Case 3. Neuron densities are higher in area p24b' in layers Va and Vb. The high density of neurons in layer Va is clear, although the many small neurons do not contribute to NFP expression (SMI32). The neurons in layer Vb are somewhat larger in this area and more of them express NFP.

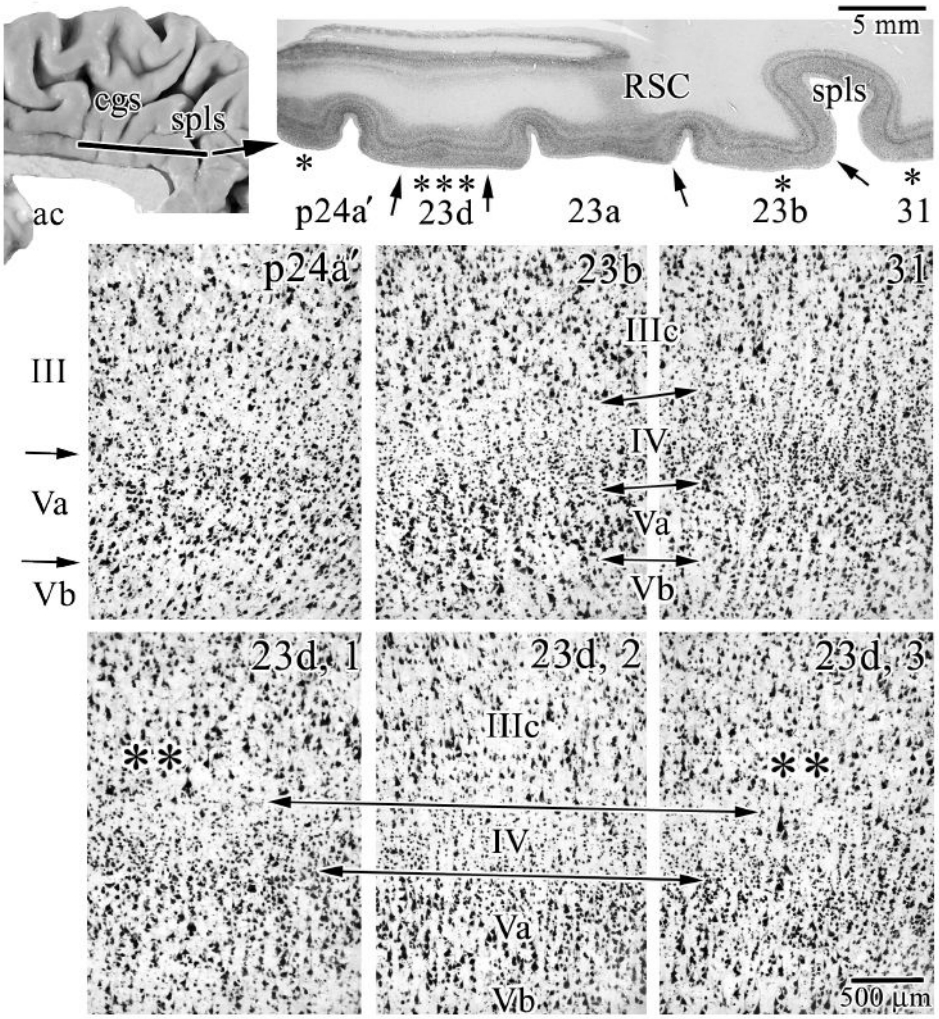

Figure 6.

Case #6 was cut in the horizontal plane and reacted for NeuN and shows the features of transition from area p24a' to area 31. The macrophotograph has an extension of retrosplenial cortex (RSC) from the callosal sulcus along the ventral border of the cingulate gyrus and marks the end of the splenium of the corpus callosum in more ventral sections. Each asterisk in this latter section shows where microphotographs were taken and the arrows indicate the borders between adjacent areas. In addition to the architectures of areas in this section, the bottom three microphotographs are of area 23d. The long double arrows delimit layer IV and adjacent layers and the double asterisks show points at which there is an intermingling of large layer IIIc and Va pyramidal neurons as is characteristic of dysgranular cortices. spls, splenial sulcus.

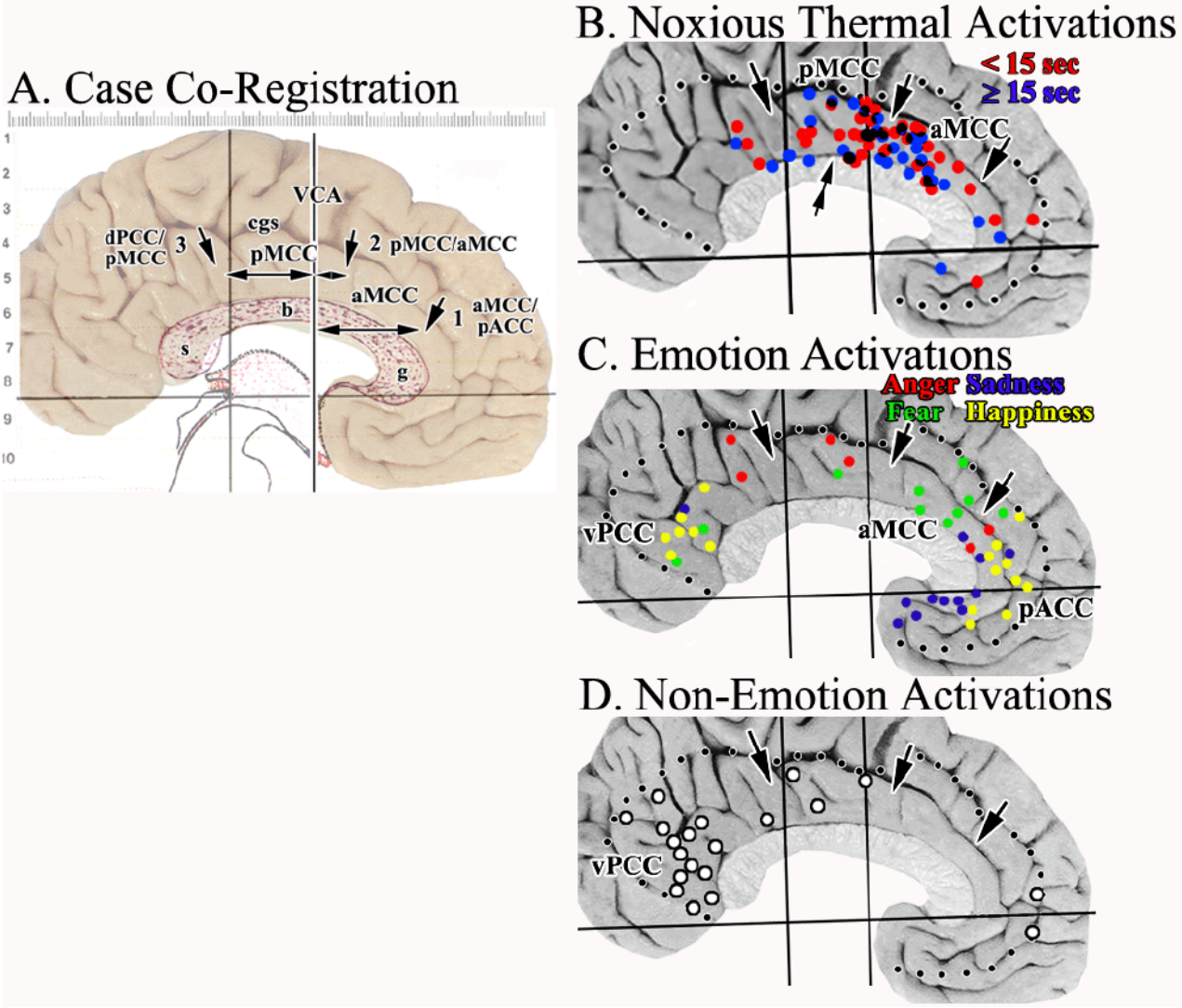

Figure 7.

A. Cytological borders of each medial surface photograph were co-registered to the Talairach and Tournoux (1988) coordinate system and corpus callosum as shown here for Case 2. Each of the borders were identified histologically (3 arrows) and measurements taken to the VCA as indicated with the double-headed arrows. B.-C. Activation sites in cingulate cortex were plotted in relation to the average coordinates for each border (dotted lines mark edge of cingulate cortex). The double arrow in B. suggests a point at which the density of sites associated mainly with short, noxious stimuli changes in the y axis. There is a striking localization of nociceptive activity in aMCC with a prominent aggregate around the VCA in pMCC. C. Most fear activity was in aMCC. D. Although Non-Emotion activity was striking in vPCC, none was in aMCC and pACC was virtually devoid of it. This suggests the latter activations are associated with processing *specific* to emotion. cgs, cingulate sulcus; g, b, s, genu, body, and splenium of the corpus callosum.

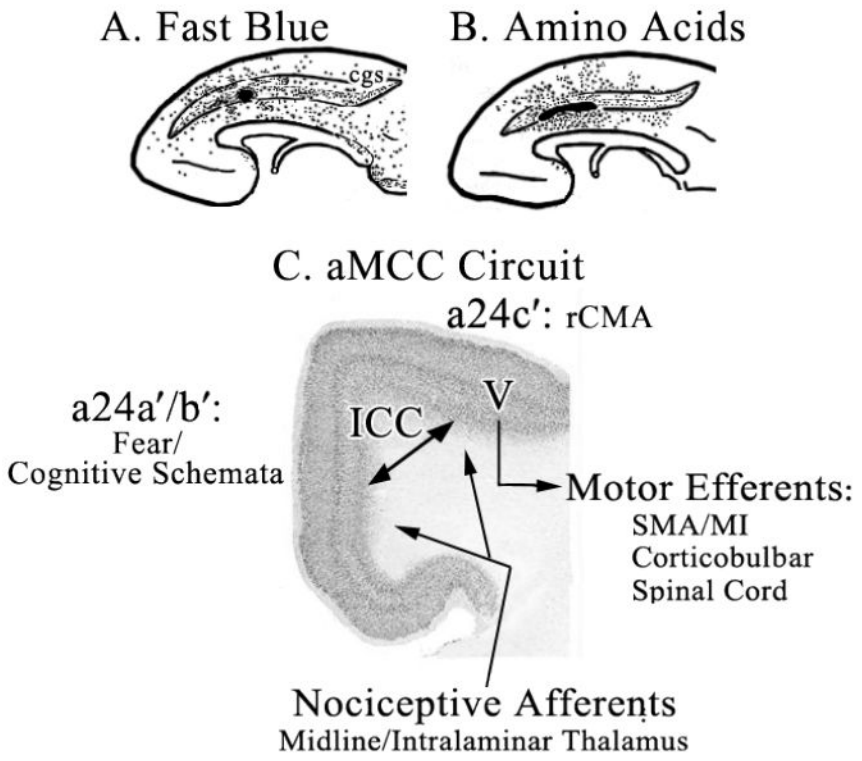

Figure 8.

Circuit derived from monkey connection studies to guide understanding of MCC functions. Retrograde labeling of neurons (A. Fast Blue; dots) and anterograde labeling of axons (B. Amino Acids; dots mark tritium-labeled terminals; modified from Van Hoesen et al., 1993) show a dense and reciprocal connection between sulcal rCMA and gyral cortex and these are indicated with a double arrow for intracingulate connections (ICC) in "C. aMCC Circuit" (coronal section from aMCC in Fig. 2). One sequence involves activation of fear/cognitive schemata in aMCC with noxious stimuli via the midline and intralaminar thalamic nuclei. This activation leads to changing behavioral responses via motor efferents (V, layer V) to prevent similar painful outcomes in the future. cgs, cingulate sulcus; MI, primary motor cortex; SMA, supplementary motor area.

Table 1

Case Characteristics

Case #	Age	Gender	Brian weight (gm)	Cause of death	Postmortem Int. (hr)
Celloidin					
1	45	M	1093	midbrain stroke	6
Frozen					
2	57	M	1360	pneumonia	3
3	57	F	1300	cancinoma, colon	20
4	52	F	1210	carcinoma, lung	15
5	44	M	1550	carcinoma, lung	9
6	59	M	1160	congestive heart failure	12
Mean±SEM	52±2.7		1279±67		10.8±2.5

Table 2

Border Coordinates from VCA

	24b/a24b'	**a24b'/p24b'**	**p24b'/23d**
Case 1	+32 mm	+7 mm	-16 mm
Case 2	+29	+7	-28
Case 3	+32	+6.5	-22
Case 4	+27	+1.5	-23
Case 5	+31	+3	-24
Case 6	+28	+2	-19
Mean±SEM	y = +30±0.9	+4.5 ±1.1	-22±1.7